HHS Public Access

Author manuscript

Biochim Biophys Acta Mol Basis Dis. Author manuscript; available in PMC 2024 February 09.

Published in final edited form as:

Biochim Biophys Acta Mol Basis Dis. 2024 January ; 1870(1): 166848. doi:10.1016/j.bbadis.2023.166848.

Therapeutic targeting of HYPDH/PRODH2 with *N*-propargylglycine offers a Hyperoxaluria treatment opportunity

Joanna Bons[a,1], **Ada Tadeo**[a,1], **Gary K. Scott**[a,1], **Fadzai Teramayi**[a], **John J. Tanner**[b], **Birgit Schilling**[a], **Christopher C. Benz**[a,*,2], **Lisa M. Ellerby**[a,*,2]

[a]Buck Institute for Research on Aging, Novato, CA, USA

[b]Departments of Biochemistry and Chemistry, University of Missouri, Columbia, MO, USA

Abstract

N-propargylglycine prevents 4-hydroxyproline catabolism in mouse liver and kidney.

N-propargylglycine is a novel suicide inhibitor of PRODH2 and induces mitochondrial degradation of PRODH2.

PRODH2 is selectively expressed in liver and kidney and contributes to primary hyperoxaluria (PH).

Preclinical evaluation of *N*-propargylglycine efficacy as a new PH therapeutic is warranted.

Keywords

4-hydroxyproline dehydrogenase (HYPDH/PRODH2); *N*-propargylglycine (*N*-PPG); 4-hydroxyproline (Hyp); Primary hyperoxaluria (PH)

The mitochondrial enzyme 4-hydroxyproline dehydrogenase (HYPDH/PRODH2) is solely responsible for the first step in the catabolism of 4-hydroxyproline (Hyp). Collagen turnover and dietary intake result in a daily load of Hyp estimated at 660 mg/d in a normal individual with the liver and, to a lesser degree, the kidneys responsible for its catabolism [1]. Glyoxylate, a highly reactive aldehyde, results from the third step in the catabolism of Hyp and, in normal circumstances, most is rapidly processed to glycine in peroxisomes or reduced to glycolate in the mitochondria or cytosol [1]. The rest is oxidized

*Corresponding authors. lellerby@buckinstitute.org (L.M. Ellerby).

[1]These authors contributed equally and share first authorship.

[2]Share senior authorship.

CRediT authorship contribution statement

Joanna Bons: Methodology, Investigation, Writing – review & editing. **Ada Tadeo:** Methodology, Investigation. **Gary K. Scott:** Conceptualization, Methodology, Investigation, Writing – original draft, Supervision. **Fadzai Teramayi:** Methodology, Investigation. **John J. Tanner:** Methodology, Investigation. **Birgit Schilling:** Methodology, Investigation, Writing – review & editing. **Christopher C. Benz:** Conceptualization, Writing – review & editing, Funding acquisition, Supervision. **Lisa M. Ellerby:** Conceptualization, Writing – review & editing, Funding acquisition, Resources, Supervision.

Declaration of competing interest

The authors have no financial/personal interest or belief that could affect their objectivity. No potential competing interests exist.

Appendix A. Supplementary data

Supplementary data to this article can be found online at https://doi.org/10.1016/j.bbadis.2023.166848.

to oxalate, an unusable end-product of mammalian metabolism that must be renally secreted to avoid the buildup of tissue-damaging calcium oxalate crystals. The failure to properly catabolize glyoxylate underlies primary hyperoxaluria (PH), a rare but debilitating set of monogenetic diseases in which abnormally high oxalate levels lead to damaging calcium oxalate deposition in the kidneys (also in the eyes, heart, skin and bone), nephrocalcinosis, and end-stage kidney failure [2].

Three genetic subtypes of PH (PH1, PH2 and PH3) have been well characterized at the molecular level. However, effective therapeutic options, short of kidney/liver transplantation, are not available, especially for PH2 and PH3. For infants and young adults born with an inborn deficiency in alanine:glyoxylate aminotransferase (AGT) characteristic of PH1, the FDA recently approved monthly injections of lumasiran (Oxlumo, Alnylam Pharmaceuticals Inc.). This small interfering ribonucleic acid (siRNA) targets the glycolate oxidase (GO) upstream of AGT and reduces urinary oxalate secretion in some but not all PH1 patients [3,4].

Molecular studies of oxalate production in PH identified Hyp catabolism by HYPDH/ PRODH2 as contributing significantly to oxalate production. In normal individuals, Hyp catabolism accounts for ~15 % of urine oxalate, but in PH1, PH2 and PH3 patients, Hyp catabolism accounts for ~18 %, ~57 % and ~ 33 %, respectively, of urinary oxalate levels [2]. A Hypdh/Prodh2 knockout (KO) mouse model had plasma Hyp levels ~20-fold higher than control mice, but a normal phenotype with urinary oxalate levels reduced 18 % relative to control male mice. More importantly, when the Hypdh/Prodh2 KO mouse was crossed with the glyoxylate reductase/hydroxypyruvate reductase (Grhpr) KO mouse, a model of PH2, the double knockout mouse had reduced hyperoxaluria and was spared development and tissue deposition of calcium oxalate crystals [5].

Our studies with the compound *N*-propargylglycine (*N*-PPG), initially undertaken for its targeting of the proline catabolizing enzyme PRODH1 to treat the protein misfolding disease, Huntington's disease (HD), serendipitously revealed that *N*-PPG targets its paralog, HYPDH/ PRODH2, thus offering possibilities for its development as a PH therapeutic.

Previous mouse studies showed that *N*-PPG penetrates the blood- brain barrier, promotes decay of Prodh1, and induces a beneficial mitohormesis response [6,7]. HD mice were utilized to determine if mitohormesis response induced by *N*-PPG treatment mitigated metabolic or disease phenotypes. To show that *N*-PPG treatment produces enhanced proline levels due to inhibition and mitochondrial decay of Prodh1 protein, metabolomic analysis was performed using kidney lysates from mice treated with *N*-PPG daily for 9 days with 50 mg/kg daily by oral gavage. The heatmap of unsupervised clustering of 20 amino acids and 21 amino acids–related metabolites in kidney samples from *N*-PPG-treated (50 mg/kg) and vehicle-treated wild-type (WT) and R6/2 (HD) mice ($N = 3$ mice per group) revealed no correlation between groups. As expected, proline levels were upregulated (Fig. 1A, WT *N*-PPG/WT VEH ratio 2.39; R6/2 *N*-PPG/R6/2 VEH ratio 1.42); but interestingly, Hyp was the most significantly upregulated metabolite in both B6 (WT) and R6/2 (HD) treated mice in kidney (Fig. 1A, WT *N*-PPG/WT VEH ratio 4.57; R6/2 *N*-PPG/R6/2 VEH ratio 2.83). In another metabolic study in R6/2 mice treated with 50 mg/kg daily by oral gavage for 14 days

(untreated, $N = 4$, *N*-PPG, $N = 5$), only Hyp was significantly upregulated in blood as shown by the bar plots (Fig. 1B, 3.59-fold increase, Q-value = 3.98e-4); whereas in brain, both Hyp (2.72-fold, Q-value = 1.62e-3) and proline (2.57-fold, Q-value = 8.15e-4) were significantly elevated (Fig. 1B). These results strongly suggested that *N*-PPG is targeting and irreversibly inhibiting both Hypdh/Prodh2 and Prodh1.

N-PPG is a unique suicide inhibitor of proline dehydrogenases. An irreversible covalent link is formed between the FAD cofactor and a conserved active site lysine residue within the enzymatic pocket [8]. Our previous study with PRODH1 demonstrated that this modification promotes degradation of the enzyme, whereas classical, reversible competitive inhibitors of PRODH1, such as proline analogs, have no effect on its mitochondrial protein levels.

HYPDH/PRODH2 is similar to PutA, the bacterial homolog of PRODH1, so it was natural to ask if *N*-PPG affects HYPDH/PRODH2 [6]. Comparing an AlphaFold model of HYPDH/PRODH2 from UniProt (Q9UF12) with PutA PRODH crystal structures revealed that the canonical PRODH $(\beta\alpha)_8$ fold and FAD binding site are conserved in HYPDH/PRODH2, consistent with HYPDH/PRODH2 being a target of *N*-PPG (Fig. 1C). Importantly, Lys236 of HYPDH/PRODH2 occupies an active site location analogous to PRODH1's Lys234. Structural modeling predicts a covalent linkage between *N*-PPG, the FAD molecule in the HYPDH/PRODH2 active site and its pocket Lys236 (Fig. 1C).

To determine if *N*-PPG affects HYPDH/PRODH2 protein levels, the human hepatocarcinoma cell line HepG2 was treated with *N*-PPG [6]. This cell line is well characterized as recapitulating Hyp catabolism by HYPDH/PRODH2 [1]. *N*-PPG treatment at 5 mM for 48 h produced a ~ 40 % reduction in HYPDH/PRODH2 expression levels (Fig. 1D). Notably, the mitochondria HYPDH/PRODH2 bands at ~55 kDa are consistent with the Hypdh/Prodh2 KO study [5], but the non-specific bands at ~75 kDa detected by our anti-HYPDH/PRODH2 antibody in the HepG2 cytoplasmic fraction are insensitive to *N*-PPG treatment. These results suggest that, as with PRODH1, the covalent interaction between *N*-PPG and HYPDH/PRODH2 promotes protein structural distortion and its mitochondrial protein degradation [6].

The increased levels of mouse Hyp induced by *N*-PPG treatment suggest a reduction in the mouse liver's Hyphd/Prohd2 catabolizing capacity. Although both liver and kidney catabolize Hyp, the liver has the major Hyp catabolizing role. Thus, Hypdh/Prodh2 liver levels exceed those of kidney by at least a factor of 40-fold accounting for the fact that the liver has four times the mass of the kidney (Fig. 1D right side). To assess *N*-PPG's effect on Hyphd/Prohd2 liver levels, B6 mice were treated at 200 mg/kg daily by oral gavage for 5 days (untreated, $N = 3$, *N*-PPG treated mice, $N = 4$). This treatment was sufficient to produce a mean reduction in Hypdh/Prohd2 liver levels to 73 % of control liver levels (Fig. 1E). Additionally, as Prodh1 is also expressed in the liver, *N*-PPG reduced mean Prodh1 levels to 66 % of control (Fig. 1E), a result consistent with our previous observation of *N*-PPG reduced Prodh1 brain expression [6].

Genetic failures in glyoxylate metabolism lead to three life-threatening PH conditions [9,10]. No effective pharmacological interventions prevent the progressive nephrocalcinosis

and eventual end-stage kidney disease. Our preliminary results show that the orally available and extremely well-tolerated drug-like small molecule, *N*-PPG, rapidly elevates Hyp levels *in vivo* as a result of reducing the liver's mitochondrial Hypdh/Prohd2 expression, a proposed target for novel PH therapeutics [5,11]. In studies not presented here but underscoring *N*-PPG's safety, WT B6 mice gavaged with 100 or 200 mg/kg daily for 8 weeks and followed for 8 weeks showed no health or behavioral differences relative to control mice (manuscript under review).

Grhpr KO mouse models were developed as tools for preclinical development of novel PH therapeutics. Thus, a significant next step would be to evaluate *N*-PPG's effectiveness in mouse models relevant to PH2 and PH3 [12,13]. Grhpr KO mice develop calcium oxalate crystals in the kidney from a failure to reduce glyoxylate to glycolate. Interestingly, these mice have threefold greater urinary oxalate levels than control mice, and males more affected than females. Yet, only ~25 % of Grhpr KO male mice developed nephrocalcinosis and the symptoms were mild [12]. However, when challenged with a 1 % Hyp diet, all Grhph KO mice presented with severe nephrocalcinosis, a condition that could be rescued by crossing into a Hypdh/Prodh2 KO background [5].

An important consideration for long-term treatment of PH2 and PH3 might be future development of a more selective inhibitor of HYPDH/ PRODH2 over PRODH1 to avoid hyperprolinemia (HP) from chronic exposure to *N*-PPG. Primary HP, as caused by a rare autosomal recessive inborn deficiency in PRODH1, is usually asymptomatic but has been linked to an increased risk of schizophrenia [14–16]. Nonetheless, given its proven safety and capacity to suppress Hyp catabolism in two other mouse models, *N*-PPG may prove to be well tolerated and capable of mitigating the hyperoxaluria and nephrocalcinosis phenotypes in mouse models of PH1 and PH2, establishing a step forward toward clinical development of a new PH therapeutic or kidney stone treatment for human use.

Supplementary Material

Refer to Web version on PubMed Central for supplementary material.

Acknowledgements

This work was supported by Elizabeth MA Stevens memorial funding (CC Benz) and "The Taube Family Program in Regenerative Medicine Genome Editing for Huntington's Disease" (LM Ellerby), USA NIH grants R01-NS100529 (LM Ellerby), U24-CA210990 (CC Benz), U54-AG075932 (CC Benz, GK Scott) and R01-GM132640 (JJ Tanner). We thank Duke University School of Medicine for use of their Proteomics and Metabolomics Core Facility which provided the metabolomic analysis of our mouse tissue samples.

Data availability

Data will be made available on request.

References

[1]. Jiang J, Johnson LC, Knight J, Callahan MF, Riedel TJ, Holmes RP, Lowther WT, Metabolism of [13C5]hydroxyproline in vitro and in vivo: implications for primary hyperoxaluria, Am. J. Physiol. Gastrointest. Liver Physiol 302 (6) (2012) G637–G643, 10.1152/ajpgi.00331.2011 (Epub 20111229). [PubMed: 22207577]

[2]. Fargue S, Milliner DS, Knight J, Olson JB, Lowther WT, Holmes RP, Hydroxyproline metabolism and oxalate synthesis in primary hyperoxaluria, J. Am. Soc. Nephrol 29 (6) (2018) 1615–1623, 10.1681/ASN.2017040390 (Epub 20180327.). [PubMed: 29588429]

[3]. Garrelfs SF, Frishberg Y, Hulton SA, Koren MJ, O'Riordan WD, Cochat P, Deschenes G, Shasha-Lavsky H, Saland JM, Van't Hoff WG, Fuster DG, Magen D, Moochhala SH, Schalk G, Simkova E, Groothoff JW, Sas DJ, Meliambro KA, Lu J, Sweetser MT, Garg PP, Vaishnaw AK, Gansner JM, McGregor TL, Lieske JC, Collaborators I-A, Lumasiran, an RNAi therapeutic for primary hyperoxaluria type 1, N. Engl. J. Med 384 (13) (2021) 1216–1226, 10.1056/NEJMoa2021712. [PubMed: 33789010]

[4]. Moya-Garzon MD, Gomez-Vidal JA, Alejo-Armijo A, Altarejos J, Rodriguez-Madoz JR, Fernandes MX, Salido E, Salido S, Diaz-Gavilan M, Small molecule-based enzyme inhibitors in the treatment of primary hyperoxalurias, J. Pers. Med 11 (2) (2021), 10.3390/jpm11020074 (Epub 20210127.).

[5]. Buchalski B, Wood KD, Challa A, Fargue S, Holmes RP, Lowther WT, Knight J, The effects of the inactivation of Hydroxyproline dehydrogenase on urinary oxalate and glycolate excretion in mouse models of primary hyperoxaluria, Biochim. Biophys. Acta Mol. basis Dis 1866 (3) (2020) 165633, 10.1016/j.bbadis.2019.165633 (Epub 20191207.).

[6]. Scott GK, Mahoney S, Scott M, Loureiro A, Lopez-Ramirez A, Tanner JJ, Ellerby LM, Benz CC, N-Propargylglycine: a unique suicide inhibitor of proline dehydrogenase with anticancer activity and brain-enhancing mitohormesis properties, Amino Acids 53 (12) (2021) 1927–1939, 10.1007/s00726-021-03012-9 (Epub 2021/06/06.). [PubMed: 34089390]

[7]. Scott GK, Yau C, Becker BC, Khateeb S, Mahoney S, Jensen MB, Hann B, Cowen BJ, Pegan SD, Benz CC, Targeting mitochondrial proline dehydrogenase with a suicide inhibitor to exploit synthetic lethal interactions with p53 upregulation and glutaminase inhibition, Mol. Cancer Ther 18 (8) (2019) 1374–1385, 10.1158/1535-7163.MCT-18-1323 (Epub 20190612.). [PubMed: 31189611]

[8]. White TA, Johnson WH Jr., C.P. Whitman, J.J. Tanner, Structural basis for the inactivation of *Thermus thermophilus* proline dehydrogenase by N-propargylglycine, Biochemistry 47 (20) (2008) 5573–5580, 10.1021/bi800055w (Epub 20080422.). [PubMed: 18426222]

[9]. Burns Z, Knight J, Fargue S, Holmes R, Assimos D, Wood K, Future treatments for hyperoxaluria, Curr. Opin. Urol 30 (2) (2020) 171–176, 10.1097/MOU.0000000000000709. [PubMed: 31895888]

[10]. Salido E, Pey AL, Rodriguez R, Lorenzo V, Primary hyperoxalurias: disorders of glyoxylate detoxification, Biochim. Biophys. Acta 1822 (9) (2012) 1453–1464, 10.1016/j.bbadis.2012.03.004 (Epub 20120314.). [PubMed: 22446032]

[11]. Summitt CB, Johnson LC, Jonsson TJ, Parsonage D, Holmes RP, Lowther WT, Proline dehydrogenase 2 (PRODH2) is a hydroxyproline dehydrogenase (HYPDH) and molecular target for treating primary hyperoxaluria, Biochem. J 466 (2) (2015) 273–281, 10.1042/BJ20141159. [PubMed: 25697095]

[12]. Knight J, Holmes RP, Cramer SD, Takayama T, Salido E, Hydroxyproline metabolism in mouse models of primary hyperoxaluria, Am. J. Physiol. Ren. Physiol 302 (6) (2012) F688–F693, 10.1152/ajprenal.00473.2011 (Epub 20111221.).

[13]. Salido EC, Li XM, Lu Y, Wang X, Santana A, Roy-Chowdhury N, Torres A, Shapiro LJ, Roy-Chowdhury J, Alanine-glyoxylate aminotransferase-deficient mice, a model for primary hyperoxaluria that responds to adenoviral gene transfer, Proc. Natl. Acad. Sci. U. S. A 103 (48) (2006) 18249–18254, 10.1073/pnas.0607218103 (Epub 20061116). [PubMed: 17110443]

[14]. Qin X, Chen J, Zhou T, 22q11.2 deletion syndrome and schizophrenia, Acta Biochim. Biophys. Sin. Shanghai 52 (11) (2020) 1181–1190, 10.1093/abbs/gmaa113. [PubMed: 33098288]

[15]. Williams HJ, Williams N, Spurlock G, Norton N, Zammit S, Kirov G, Owen MJ, O'Donovan MC, Detailed analysis of PRODH and PsPRODH reveals no association with schizophrenia, Am. J. Med. Genet. B Neuropsychiatr. Genet 120B (1) (2003) 42–46, 10.1002/ajmg.b.20049. [PubMed: 12815738]

[16]. Willis A, Bender HU, Steel G, Valle D, PRODH variants and risk for schizophrenia, Amino Acids 35 (4) (2008) 673–679, 10.1007/s00726-008-0111-0 (Epub 20080605). [PubMed: 18528746]

[17]. Adams KJ, Pratt B, Bose N, Dubois LG, St John-Williams L, Perrott KM, Ky K, Kapahi P, Sharma V, MacCoss MJ, Moseley MA, Colton CA, MacLean BX, Schilling B, Thompson JW, Alzheimer's Disease Metabolomics C. Skyline for Small Molecules: A Unifying Software Package for Quantitative Metabolomics, J. Proteome Res 19 (4) (2020) 1447–1458, 10.1021/acs.jproteome.9b00640 (Epub 20200326). [PubMed: 31984744]

[18]. Pang Z, Chong J, Zhou G, de Lima Morais DA, Chang L, Barrette M, Gauthier C, Jacques PE, Li S, Xia J, MetaboAnalyst 5.0: narrowing the gap between raw spectra and functional insights, Nucleic Acids Res. 49 (W1) (2021), 10.1093/nar/gkab382 (W388-W96).

[19]. Korasick DA, Singh H, Pemberton TA, Luo M, Dhatwalia R, Tanner JJ, Biophysical investigation of type A PutAs reveals a conserved core oligomeric structure, FEBS J. 284 (18) (2017) 3029–3049, 10.1111/febs.14165 (Epub 20170801). [PubMed: 28710792]

[20]. Srivastava D, Zhu W, Johnson WH Jr., C.P. Whitman, D.F. Becker, J.J. Tanner, The structure of the proline utilization a proline dehydrogenase domain inactivated by N-propargylglycine provides insight into conformational changes induced by substrate binding and flavin reduction, Biochemistry 49 (3) (2010) 560–569, 10.1021/bi901717s. [PubMed: 19994913]

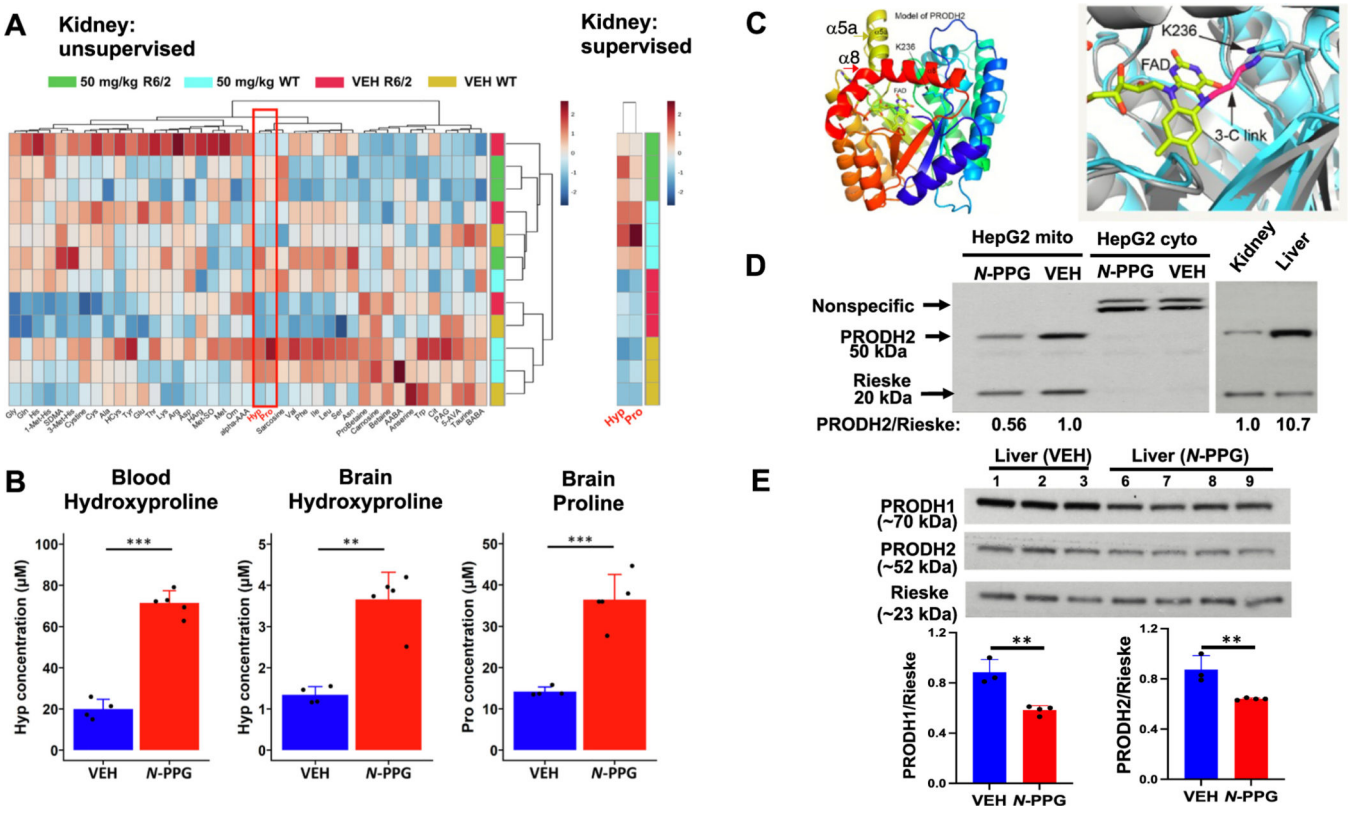

Fig. 1.

N-PPG targets HYPDH/PRODH2 modulating 4-hydroxyproline levels. a) Left, unsupervised clustering of 20 amino acids and 21 amino acids–related metabolites using kidney samples from *N*-PPG-treated (50 mg/kg) and vehicle-treated wild-type (WT) and R6/2 mice (*N* = 3 mice per group). Heatmap of metabolite levels using log10-transformed concentrations determined using the Biocrates MxP Quant 500 kit. Color scale bar represents z-score values after normalization. Red box highlights proline and 4-hydroxproline (Hyp) as the most differentially altered levels between *N*-PPG-treated and vehicle mice. Right, supervised clustering of hydroxyproline and proline also shows that these metabolites were up-regulated in *N*-PPG-treated *vs* vehicle-treated wild-type (WT) and R6/2 mice. Differences were significant for both hydroxyproline and proline, with a false-discovery rate (FDR) of 3.34 e-2 as determined using one-way ANOVA analysis and Fisher's LSD post-hoc testing. Metabolites include β-aminobutyric acid, taurine, 5-aminovaleric acid, phenylacetylglycine, citrulline, Trp, anserine, α-aminobutyric acid, betaine, carnosine, proline betaine, Asn, Ser, Leu, Ile, Phe, Val, sarcosine, Pro, t-OH-pro, α-aminoadipic acid, ornithine, Met, methionine sulfoxide, homoarginine, Asp, Arg, Lys, Thr, Glu, Tyr, homocysteine, Ala, Cys, Cystine, 3-methylhistidine, symmetric dimethylarginine, 1-methylhistidine, His, Gln, and Gly. The ultra-performance liquid chromatography–tandem mass spectrometry (UPLC-MS/MS) output data were imported into Skyline-daily for peak integration, calibration, and concentration calculations [17]. Exported data from Skyline were processed using a custom visual basic macro for importing into MetIDQ software (Biocrates AG) and MetaboAnalyst 5.0 [18].

b) Metabolomic analysis comparing blood and whole brains from R6/2 mice treated for 14 days with 50 mg/kg *N*-PPG or vehicle (VEH) as in panel a. Bar plots display the averaged metabolite concentration obtained in *N*-PPG-treated mice ($N = 5$) and VEH-treated mice ($N = 4$). For blood, only 4-hydroxyproline was significantly up-regulated upon *N*-PPG treatment, while in brain lysates, both proline and hydroxyproline were significantly up-regulated. Statistical analysis was performed using two-sample *t*-test followed by *p*-value correction for multiple testing. *FDR ≤ 0.05, ** FDR ≤ 0.01, *** FDR ≤ 0.001. The error bars correspond to the standard deviation. Metabolite concentrations are expressed in μM. c) To determine if the predicted active site structure of HYPDH/PRODH2 is consistent with the covalent inactivation mechanism of *N*-PPG, the AlphaFold model of HYPDH/PRODH2 was superimposed onto the crystal structure of an *N*-PPG inactivated PutA PRODH domain [19]. This modeling showed that HYPDH/PRODH2 is predicted to have a structure needed for both binding of *N*-PPG in the substrate pocket and subsequent mechanistic steps (bond breaking and formation), leading to covalent linking of the FAD N5 atom to ε-amino group of the conserved active site lysine (Lys236 in HYPDH/PRODH2) [8,20]. HYPDH/PRODH2 molecular structure accommodates *N*-PPG binding and inhibition. Structural model of HYPDH/PRODH2 from AlphaFold2 viewed looking down the enzymatic $(\beta\alpha)_8$ barrel structure using a rainbow coloring scheme with blue at the N-terminus and red at the C-terminus. The *N*-PPG covalently interacting elements FAD (yellow) and Lys236 are noted. Two unique α-helices, α8 (red) and α5a (yellow), distinguish the HYPDH/PRODH2 barrel from other $(\beta_\alpha)_8$ barrel proteins. Superposition of the HYPDH/PRODH2 model (cyan) with the crystal structure of an *N*-PPG-inactivated bacterial PRODH (PDB ID 5UR2, gray) showing that Lys236 has the potential for covalent linkage to the FAD upon inactivation by *N*-PPG with *N*-PPG's 3 carbon link (3-C link) between the bacterial PRODH's FAD and lysine shown in red. d) Western blot probed with HYPDH/PRODH2 and Rieske (for normalization) of mitochondria (mito) and cytoplasmic (cyto) fractions from HepG2 cells treated for 48 h with 5 mM *N*-PPG (+*N*-PPG) or untreated. Arrows indicate HYPDH/PRODH2 and Rieske bands. Non-specific bands are seen only in the cytoplasmic fraction that contains no signal from the mitochondrial HYPDH/PRODH2 (left). Western blot using mouse WT lysates from whole kidney and whole liver probed for Hypdh/Prodh2 with normalization to Rieske (right). e) Western blot of whole-liver lysates probed for Prodh1 and Hypdh/Prodh2 with Rieske normalization. Quantification of the Prodh1 and Hypdh/Prodh2 levels normalized to Rieske are shown in the lower panel. **, $p = 0.0025$ and 0.0076 for Prodh1 and Hypdh/Prodh2, respectively.